Lithium–Oxygen Batteries

DOI: 10.1002/anie.201100879

Oxygen Reactions in a Non-Aqueous Li^+ Electrolyte**

*Zhangquan Peng, Stefan A. Freunberger, Laurence J. Hardwick, Yuhui Chen, Vincent Giordani, Fanny Bardé, Petr Novák, Duncan Graham, Jean-Marie Tarascon, and Peter G. Bruce**

Oxygen (O_2) reduction is one of the most studied reactions in chemistry.[1] Widely investigated in aqueous media, O_2 reduction in non-aqueous solvents, such as CH_3CN, has been studied for several decades.[2–7] Today, O_2 reduction in non-aqueous Li^+ electrolytes is receiving considerable attention because it is the reaction on which operation of the Li–air (O_2) battery depends.[8–29] The Li–O_2 battery is generating a great deal of interest because theoretically its high energy density could transform energy storage.[8,9] As a result, it is crucial to understand the O_2 reaction mechanisms in non-aqueous Li^+ electrolytes. Important progress has been made using electrochemical measurements including recently by Laoire et al.[29] No less than five different mechanisms for O_2 reduction in Li^+ electrolytes have been proposed over the last 40 years based on electrochemical measurements alone.[25–29] The value of using spectroelectrochemical methods is that they can identify directly the species involved in the reaction. Here we present in situ spectroscopic data that provide direct evidence that LiO_2 is indeed an intermediate on O_2 reduction, which then disproportionates to the final product Li_2O_2. Spectroscopic studies of Li_2O_2 oxidation demonstrate that LiO_2 is not an intermediate on oxidation, that is, oxidation does not follow the reverse pathway to reduction.

In this work CH_3CN was used as the solvent because it has been used widely for O_2 reduction and shown to be sufficiently stable towards reduced O_2 species for the studies undertaken herein.[4,5] Au was chosen as the electrode because it is an excellent substrate for surface enhanced Raman spectroscopy (SERS).[30] To confirm that the electrode/electrolyte combination used herein is sufficiently stable for our studies, cyclic voltammograms (CVs) were collected in 0.1 M nBu$_4$NClO$_4$-CH_3CN saturated with O_2 at an Au electrode (Figure S1 in the Supporting Information). These data show that $Q_A/Q_C \approx 1$ (Q is the charge passed on the anodic (A) and cathodic (C) sweeps, see Table S1) at all scan rates in Figure S1, in accord with the reversibility and hence stability of the electrolyte and electrode towards the reduced O_2 species.

O_2^- has been detected previously in CH_3CN.[4] To confirm its formation on reduction of O_2 in our experiments, in situ SERS data were collected on the Au electrode in 0.1 M nBu$_4$NClO$_4$-CH_3CN at various potentials on reduction and oxidation, indicating respectively the formation of O_2^- and its disappearance (Figure 1). The peak assignments in Figure 1 were based on the vibrational spectrum for O_2^-[4a] and the SERS spectrum in Figure S2; the data for the latter were obtained by dissolving KO_2, using a crown ether to complex the K^+ and hence promote dissolution (see caption to Figure S2). The CVs of O_2 reduction as a function of scan rate were analyzed using the DigiSim software.[31] The heterogeneous rate constant, $k^0 = 2.1 \times 10^{-4}\,cm\,s^{-1}$, was obtained from this analysis. The O_2 concentration $[O_2] = 6.8$ mM and O_2 diffusion coefficient $D_{O_2} = 7.0 \times 10^{-5}\,cm^2\,s^{-1}$

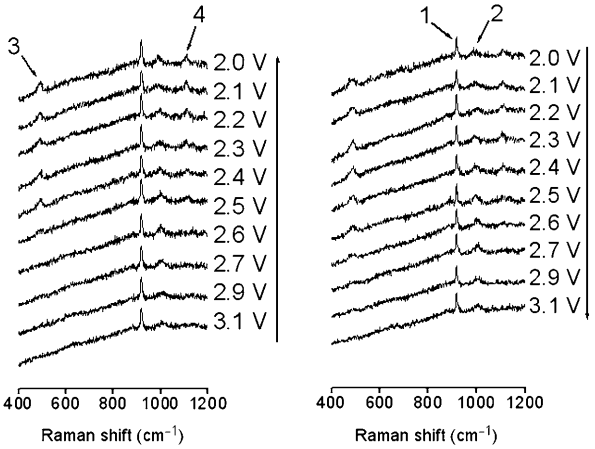

Figure 1. In situ SERS of superoxide. Spectra were obtained from a roughened Au electrode in O_2 saturated 0.1 M nBu$_4$NClO$_4$-CH_3CN. The cathodic potential sweep from 3.1 V to 2.0 V vs Li/Li^+ is shown on the left, while the anodic sweep is shown on the right. Peak assignments are as follows: 1) C–C stretch of CH_3CN at 918 cm^{-1}, 2) N–$(C_4)_4$ stretch of nBu$_4N^+$ at 996 cm^{-1}, 3) Au–O stretch of adsorbed O_2^- at 491 cm^{-1}, 4) O–O stretch of adsorbed O_2^- at 1109 cm^{-1}.

[*] Dr. Z. Peng, Dr. S. A. Freunberger, Dr. L. J. Hardwick, Y. Chen, Dr. V. Giordani, Prof. P. G. Bruce
School of Chemistry, University of St Andrews
The Purdie Building, North Haugh, St Andrews KY16 9ST (UK)
Fax: (+44) 1334-463-808
E-mail: p.g.bruce@st-andrews.ac.uk
Dr. V. Giordani, Prof. J.-M. Tarascon
Laboratoire de Réactivité et Chimie des Solides, UMR 6007
Université de Picardie Jules Verne, 80039 Amiens (France)
Dr. F. Bardé
Toyota Motor Europe, Technical Centre
Hoge Wei 33 B, B-1930 Zaventem (Belgium)
Prof. Dr. P. Novák
Electrochemistry Laboratory, Paul Scherrer Institut
CH-5232 Villigen PSI (Switzerland)
Prof. D. Graham
Department of Pure and Applied Chemistry, University of Strathclyde, 295 Cathedral Street, Glasgow, G1 1XL (UK)

[**] P.G.B. is indebted to the EPSRC, EU, and Toyota Motor Europe for financial support.

Supporting information for this article is available on the WWW under http://dx.doi.org/10.1002/anie.201100879.

were obtained by fitting the current response to a potential step at an Au microelectrode (Figure S3) following the procedure described previously[7] (see Experimental Section). It is known that O_2^- can form ion pairs with molecular cations such as organic ammonium ions, however, such interactions are weak compared with those involving Li^+ ions.[2,26]

The reaction between O_2^- and Li^+ was investigated as a function of Li^+ concentration (Figure 2). Addition of a 1 mM concentration of Li^+ resulted in the appearance of a new

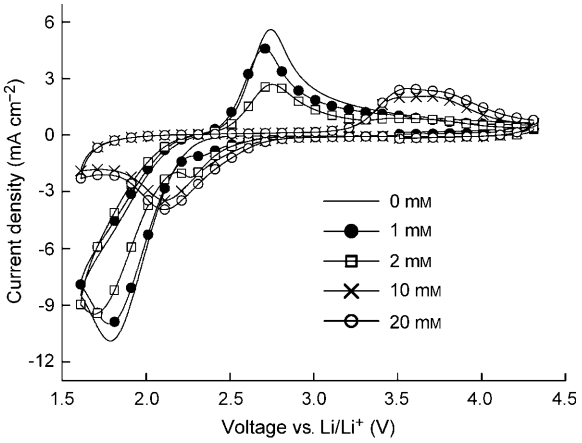

Figure 2. Cyclic voltammetry at an Au electrode in O_2-saturated 0.1 M nBu$_4$NClO$_4$-CH$_3$CN containing various concentrations of LiClO$_4$ as indicated. The scan rate was 1.0 V s^{-1} because at this rate the reduction to O_2^- and LiO_2 as a function of Li^+ concentration can be seen most clearly.

reduction peak at higher potentials (2.35 V) compared with the original O_2 reduction peak. The magnitude of the new peak grows with increasing Li^+ concentration and at the expense of the area under the original O_2 reduction peak. This behavior is consistent with an EC mechanism, that is, electrochemical reduction followed by a chemical step.[32] Such following chemical reactions severely deplete the concentration of O_2^- thus shifting the potential to higher voltages, as observed here.[32] When the concentration of Li^+ ions is lower than O_2, then there is insufficient Li^+ to react with all the O_2^- that is generated, hence "unbond" O_2^- persists and two peaks are apparent. When the concentration of Li^+ exceeds that of O_2 (in this case the O_2 concentration is 6.8 mM) then all the O_2^- is consumed by reacting with Li^+. The low voltage reduction peak disappears leaving only one reduction peak. For a similar reason the peak at 2.75 V associated with O_2^- oxidation disappears when the Li^+ concentration exceeds that of O_2. The shift of the reduction potentials to lower voltages and the lowering of the reduction current with increasing Li^+ concentration are consistent with partial blockage of the electrode surface by the insulating reduction products, which becomes more severe at higher Li^+ concentrations. Such a phenomenon has been observed before.[27] As stated above, Au was used because it permits SERS studies of the electrode surface. The same electrochemical reactions occur on glassy carbon electrodes, as shown in Figure S4.

Although these and previous electrochemical studies are very valuable, they cannot identify directly the species formed on reduction. This is illustrated by the fact that different authors have proposed different mechanisms for O_2 reduction based on electrochemical measurements;[25–29] two examples are given here:

$$O_2 + e^- \rightarrow O_2^- \quad (1a)$$

$$2\,O_2^- \leftrightarrow O_2 + O_2^{2-} \xrightarrow{2Li^+} Li_2O_2 \quad (1b)$$

or

$$O_2 + e^- \rightarrow O_2^- \quad (2a)$$

$$O_2^- + Li^+ \rightarrow LiO_2 \quad (2b)$$

$$2\,LiO_2 \rightarrow Li_2O_2 + O_2 \quad (2c)$$

Spectroscopic methods can identify directly the reaction products and their intermediates, and therefore are invaluable in investigating the O_2 reduction mechanism. The results of in situ SERS measurements are presented in Figure 3. A

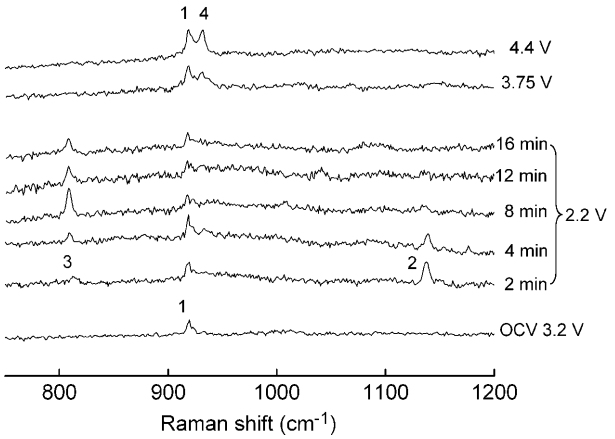

Figure 3. In situ SERS during O_2 reduction and re-oxidation on Au in O_2-saturated 0.1 M LiClO$_4$-CH$_3$CN. Spectra collected at a series of times and at the reducing potential of 2.2 V versus Li/Li$^+$ followed by other spectra at the oxidation potentials shown. The peaks are assigned as follows: 1) C–C stretch of CH$_3$CN at 918 cm^{-1}, 2) O–O stretch of LiO_2 at 1137 cm^{-1}, 3) O–O stretch of Li_2O_2 at 808 cm^{-1}, 4) Cl–O stretch of ClO_4^- at 931 cm^{-1}.

background spectrum was collected before application of a potential to the cell (OCV; open circuit voltage). The spectrum is consistent with that expected for CH$_3$CN; the peak (1) at 918 cm^{-1} is assigned to the C–C symmetric stretch in CH$_3$CN. Data were then collected at a potential of 2.2 V, that is, within the reduction peak in Figure 2. Spectra are shown at this potential for successive time intervals. Within a short time, two new peaks (2 and 3) appear that were not present at OCV. The most prominent occurs at 1137 cm^{-1} and is associated with the O–O stretch of LiO_2.[33,34] The smaller peak at 808 cm^{-1} corresponds to the O–O stretch of adsorbed Li_2O_2.[35,36] With the passage of time the LiO_2 peak diminishes until only the Li_2O_2 peak remains. The LiO_2 peak occurs some

28 cm^{-1} higher than O_2^- in nBu_4N^+ solution, in accord with the stronger binding of O_2^- to Li^+ in LiO_2, resulting in the transfer of anti-bonding electron density from $O{-}O^-$ to Li^+. The Raman spectra provided direct spectroscopic evidence that reduction of O_2 in the presence of Li^+ ions in a non-aqueous electrolyte first forms O_2^- that then binds to Li^+ forming LiO_2 on the surface of the electrode. They further demonstrate that LiO_2 is unstable and disproportionates to the more stable Li_2O_2, that is, $2\,LiO_2 \rightarrow Li_2O_2 + O_2$. In other words the Raman spectra have shown that the process of O_2 reduction in the presence of Li^+ follows Equations (2a–c) described above, and *does not* proceed through disproportionation of superoxide to peroxide ions [Equations (1a,b)] followed by the formation of Li_2O_2 without passing through LiO_2 as an intermediate.[25–29] It also shows that the LiO_2 intermediate is present on the electrode surface. It is known that on extending the voltage range to much more cathodic potentials further reduction process occurs that may be assigned to O_2^- reduction to O_2^{2-} in the absence of Li^+.[2,3] In the presence of Li^+, LiO_2 reduction to Li_2O_2 occurs (Figure S5). However, this is at a significantly more negative (lower) potential than the SERS data (0.8 V lower), thus direct reduction of LiO_2 to Li_2O_2 is unlikely to make a major contribution to the transformation of LiO_2 to Li_2O_2 at the voltages used in our experiments, which instead are dominated by disproportionation.

Returning to the CVs in Figure 2, at high Li^+ concentrations two oxidation peaks are apparent at 3.55 and 3.75 V. To investigate the oxidation in more detail, a series of CVs was collected in 0.1 M $LiClO_4$-CH_3CN (Figure 4). Each CV

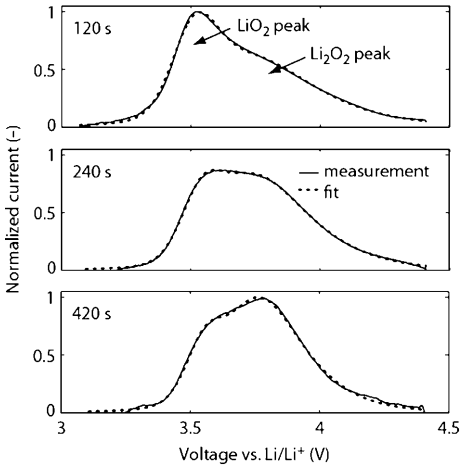

Figure 4. Oxidation waves on Au in 0.1 M $LiClO_4$-CH_3CN after various dwelling times at OCV. Before the dwelling, the potential was swept from 3.2 V to 2.2 V to form the reduction products, LiO_2 and Li_2O_2, scan rate 1.0 Vs^{-1}.

was collected by first sweeping the potential from 3.2 V (OCV) to 2.2 V and then keeping the potential at OCV for various dwell times, before completing the oxidation sweep. Sweeping the potential to 2.2 V results in the formation of LiO_2 and Li_2O_2. Thereafter, short dwell times lead to the presence of the lower voltage oxidation process, whereas this peak diminishes as the high voltage peak grows with increasing dwell time. The lower voltage oxidation peak is associated with the oxidation of LiO_2, whereas longer dwell times result in a proportionately greater quantity of Li_2O_2, the decomposition of which is associated with the high voltage oxidation peak. The purpose of the dwell time experiments was to investigate the kinetics of disproportionation: by employing various dwell times and deconvoluting the areas under the two oxidation peaks (see Experimental Section), the first-order rate constant for the disproportionation reaction from LiO_2 to $Li_2O_2 + O_2$ was calculated, $k = 2.9 \times 10^{-3}\ s^{-1}$.

The presence of oxidation peaks for both LiO_2 and Li_2O_2 in the CVs only occurs because of the relatively short time scales. In practice, Li–O_2 cells are charged and discharged over much longer times, and hence all the LiO_2 will have disproportionated to Li_2O_2 by the end of discharge. Therefore, in the context of the Li–O_2 battery, it is interesting to examine the oxidation (charging) of pure Li_2O_2. As for reduction, different mechanisms may be proposed for oxidation of Li_2O_2; for example one mechanism involves the oxidation of Li_2O_2 to LiO_2 then to O_2 [Equations (3a,b)], but others are also possible, such as Equation (4), which does not involve LiO_2 as an intermediate.

$$Li_2O_2 \rightarrow LiO_2 + Li^+ + e^- \quad (3a)$$

$$LiO_2 \rightarrow O_2 + Li^+ + e^- \quad (3b)$$

or

$$Li_2O_2 \rightarrow O_2 + 2\,Li^+ + 2\,e^- \quad (4)$$

As noted above, the oxidation peak for Li_2O_2 occurs at 3.75 V, which is above the oxidation potential for LiO_2 at 3.5 V, leading us not to expect LiO_2 as an intermediate on oxidizing Li_2O_2 since LiO_2 would be unstable at 3.75 V. However, to explore this directly, in situ SERS and in situ differential electrochemical mass spectroscopy (DEMS) data were obtained. Considering first the Raman data: after applying a reducing potential of 2 V until only Li_2O_2 was present, the potential was switched to 3.75 V (the oxidation potential of Li_2O_2) then to 4.4 V. The SERS spectra collected at these oxidation potentials are shown in Figure 3, and there is no evidence of LiO_2, consistent with Li_2O_2 decomposing directly without passing through LiO_2 as an intermediate. It has recently been confirmed that O_2^- reacts strongly with propylene carbonate electrolytes to form various decomposition products including CO_2.[37] As a result we can now use this electrolyte as a chemical probe for superoxide: if oxidation of Li_2O_2 formed LiO_2 or O_2^- then in PC electrolyte CO_2 would be observed. An electrode was constructed in the discharged state, that is, containing Li_2O_2 (Aldrich), then placed in contact with a 0.1 M solution of $LiPF_6$ in propylene carbonate. The electrode was charged in successive current steps, the results are presented in Figure S6. As the current is increased there is an immediate increase in the cell potential and a corresponding increasing in the $m/z = 32$ signal due to O_2 evolution on decomposing Li_2O_2 upon charging. No other gases are evolved at a level greater than 1% of the O_2. In

particular, the absence of a mass signal at $m/z = 44$, corresponding to CO_2, indicates that Li_2O_2 decomposes directly in a one-step process to $Li^+ + e^- + O_2$, that is, through Reaction (4). O_2 evolution upon charging Li_2O_2 has been reported earlier,[11] however, the sensitivity of the former DEMS apparatus did not allow the detection of minority gases. Here we have used a new generation of DEMS apparatus (developed by one of us; P.N.), with gas detection limits improved to low ppm values thus making possible detection of CO_2, and hence superoxide (if present), down to a level of 0.1% of O_2. Together, the SERS and DEMS results demonstrate that oxidation occurs by direct decomposition according to the reaction $Li_2O_2 \rightarrow 2Li^+ + 2e^- + O_2$. In other words, the pathways followed on reduction and oxidation are different. This is in accord with the different voltages for charge and discharge, the separation of which persists even at low charge/discharge rates as confirmed by the CV with low scan rate in Figure S7. The different pathways for reduction and oxidation do not violate the principle of microscopic reversibility. The discharge reaction is in three steps and may be viewed as an ECC mechanism [Equations (2a–c)]. For microscopic reversibility, the reaction on charging would have to reverse along the same path, that is, CCE. As reduction occurs at 2.2 V and oxidation of Li_2O_2 at approximately 3.7 V, even at low rates, as discussed above, this implies that at least one of the forward reaction steps, most likely reaction step (2c), is irreversible or at least the reverse chemical reaction is very slow. As a result, direct electrochemical oxidation of Li_2O_2 occurs more readily than reversing along the same pathway as reduction. This phenomenon has been discussed before, all be it in quite different systems such as reductive decomposition of alkylhalides.[38]

In conclusion, in situ spectroscopic studies of O_2 reduction in non-aqueous solvent, in the presence and absence of Li^+ ions, have provided direct evidence of LiO_2 as an intermediate on O_2 reduction, which then disproportionates to Li_2O_2 ($k_{dispr.} = 2.9 \times 10^{-3}\ s^{-1}$). On charging, in situ spectroscopic studies reveal that Li_2O_2 decomposes directly, in a one-step reaction to evolve O_2 and does not pass through LiO_2 as an intermediate.

Experimental Section

CH_3CN was distilled then further dried for several days over freshly activated molecular sieves (type 4 Å) resulting a final water content of ≤ 4 ppm (determined using a Mettler-Toledo Karl Fischer titration apparatus). Electrochemical grade nBuNClO$_4$ and battery grade $LiClO_4$ were used for preparing the electrolytes as they can be obtained in high purity. Prior to use, both nBuNClO$_4$ and $LiClO_4$ were dried by heating under vacuum at 80 and 160 °C, respectively, for 24 h. Electrochemical measurements were conducted in a multi-necked, air-tight glass cell with valves to control the gas inlet and outlet. A polycrystalline Au disk (BAS Inc.) electrode (diameter 1.6 mm or 10 μm for ultra-microelectrode) was used as the working electrode and was polished with 0.05 μm alumina slurry prior to use. The surface area of the ultra-micro Au working electrode was quantified by steady state polarization in 0.5 M nBuNBF$_4$-CH_3CN containing 1.0 mM ferrocene (Fc) using the known diffusion coefficient, $D = 1.7 \times 10^{-5}\ cm^2 s^{-1}$, for Fc.[39a] Diffusion coefficient and solubility of O_2 was extracted from the potential step at an Au microelectrode using the nonlinear curve fitting function in Origin 6.1 (Originlab Co.) following the equations proposed by Shoup and Szabo.[39b] A platinum wire served as the counter electrode. A silver wire immersed in a glass tube containing the supporting electrolyte, separated from the main solution by a porous glass frit, was used as the quasi reference electrode, which was calibrated with the Fc^+/Fc couple, itself calibrated versus Li/Li^+(1.0 M) in propylene carbonate (PC). Electrochemical measurements were carried out at room temperature using an Autolab PG30 electrochemical workstation. Deconvolution of the two oxidation peaks for the dwell time experiments was carried out using customized code written within the Matlab software package. A linear combination of Gaussian and Cauchy distributions was used to describe the peaks. The background was determined by an oxidation sweep without prior reduction sweep.

The electrochemically roughened Au working electrode[40] was placed behind a 1 mm thick sapphire window with the reference and counter electrodes identical to those described above. Raman spectra were recorded using a customized Renishaw Raman system with an excitation wavelength of 632.8 nm. The collection optics is based on a Leica inverted microscope with a 50× objective lens. The power of the laser beam delivered to the electrode surface is estimated to be 2.5 mW and the spectrum acquisition time is typically 30 s.

The cell exploring charging of chemical Li_2O_2 consisted of a lithium anode, electrolyte (0.1 M $LiPF_6$ in PC) impregnated into a glass fiber separator, and a porous cathode containing the Li_2O_2. The porous cathode consisted of carbon black (Super P, TIMCAL), α-MnO_2 nanowires, polyvinylidenefluoride (Kynar) (mol ratios of 95:2.5:2.5) and chemical Li_2O_2. The cell was purged continuously with Ar gas which flowed from the cell into the mass spectrometer carrying the evolved gases for mass analysis. The experiment setup is described in detail elsewhere.[41]

Received: February 3, 2011
Revised: April 4, 2011
Published online: May 25, 2011

Keywords: electrochemistry · lithium batteries · oxygen · reduction · surface enhanced Raman spectroscopy

[1] "Oxygen Electrochemistry": M. R. Tarasevich, A. Sadkowski, E. Yeager in *Comprehensive Treatise in Electrochemistry* (Eds.: J. O. M. Bockris, B. E. Conway, E. Yeager, S. U. M. Khan, R. E. White), Plenum, New York, **1983**, pp. 301 – 399.
[2] D. T. Sawyer, J. L. Robert, Jr., *J. Electroanal. Chem.* **1966**, *12*, 90.
[3] D. T. Sawyer, *Oxygen Chemistry*, Oxford University Press, Oxford, **1991**, chap. 2.
[4] a) D. Vasudevan, H. Wendt, *J. Electroanal. Chem.* **1995**, *392*, 69; b) M. E. Peover, B. S. White, *J. Chem. Soc. Chem. Commun.* **1965**, 183; c) M. E. Peover, B. S. White, *Electrochim. Acta* **1966**, *11*, 1061; d) T. A. Lorenzola, B. A. López, M. C. Giordono, *J. Electrochem. Soc.* **1983**, *130*, 1359.
[5] C. Shi, F. C. Anson, *J. Electroanal. Chem.* **2000**, *484*, 69.
[6] M. M. Islam, T. Ohsaka, *J. Phys. Chem. C* **2008**, *112*, 1269.
[7] a) R. G. Evans, O. V. Klymenko, S. A. Saddoughi, C. Hardacre, R. G. Compton, *J. Phys. Chem. B* **2004**, *108*, 7878; b) X.-J. Huang, E. I. Rogers, C. Hardacre, R. G. Compton, *J. Phys. Chem. B* **2009**, *113*, 8953.
[8] J.-S. Lee, S. T. Kim, R. Cao, N.-S. Choi, M. Liu, K. T. Lee, J. Cho, *Adv. Energy. Mater.* **2011**, *1*, 34.
[9] G. Girishkumar, B. McCloskey, A. C. Luntz, S. Swanson, W. Wilcke, *J. Phys. Chem. Lett.* **2010**, *1*, 2193.
[10] K. M. Abraham, Z. Jiang, *J. Electrochem. Soc.* **1996**, *143*, 1.
[11] T. Ogasawara, A. Débart, M. Holzapfel, P. Novák, P. G. Bruce, *J. Am. Chem. Soc.* **2006**, *128*, 1390.
[12] A. Débart, A. J. Paterson, J. Bao, P. G. Bruce, *Angew. Chem.* **2008**, *120*, 4597; *Angew. Chem. Int. Ed.* **2008**, *47*, 4521.

[13] N. Imanishi, S. Hasegawa, T. Zhang, A. Hirano, Y. Takeda, O. Yamamoto, *J. Power Sources* **2008**, *185*, 1392.
[14] S. J. Visco, B. D. Katz, Y. S. Nimon, L. D. DeJonghe, U.S. Pat. 7,282,295, **2007**.
[15] S. Lee, S. Zhu, C. C. Milleville, C.-Y. Lee, P. Chen, K. J. Takeuchi, E. S. Takeuchi, A. C. Marschilok, *Electrochem. Solid-State Lett.* **2010**, *13*, A162.
[16] X.-H. Yang, P. He, Y.-Y. Xia, *Electrochem. Commun.* **2009**, *11*, 1127.
[17] W. Xu, J. Xiao, D. Wang, J. Zhang, J.-G. Zhang, *Electrochem. Solid-State Lett.* **2010**, *13*, A48.
[18] J. Read, *J. Electrochem. Soc.* **2002**, *149*, A1190.
[19] A. K. Thapa, K. Saimen, T. Ishihara, *Electrochem. Solid-State Lett.* **2010**, *13*, A165.
[20] G. Q. Zhang, J. P. Zheng, R. Liang, C. Zhang, B. Wang, M. Hendrickson, E. J. Plicha, *J. Electrochem. Soc.* **2010**, *157*, A953.
[21] T. Kuboki, T. Okuyama, T. Ohsaki, N. Takami, *J. Power Sources* **2005**, *146*, 766.
[22] Y. G. Wang, H. S. Zhou, *J. Power Sources* **2010**, *195*, 358.
[23] S. D. Beattie, D. M. Manolescu, S. L. Blair, *J. Electrochem. Soc.* **2009**, *156*, A44.
[24] J. S. Hummelshoj, S. Blomqvisy, S. Datta, T. Vegge, J. Rossmeisl, K. S. Thygesen, A. C. Luntz, *J. Chem. Phys.* **2010**, *132*, 071101.
[25] T. Fujinaga, S. Sakara, *Bull. Chem. Soc. Jpn.* **1974**, *47*, 2781.
[26] D. T. Sawyer, G. Chiericato, C. T. Angelis, E. J. Nanni, T. Tsuchiya, *Anal. Chem.* **1982**, *54*, 1720.
[27] D. Aurbach, M. Daroux, P. Faguy, E. Yeager, *J. Electroanal. Chem.* **1991**, *297*, 225.
[28] Y.-C. Lu, H. A. Gasteiger, E. Crumlin, R. McGuire, Y. Shao-Horn, *J. Electrochem. Soc.* **2010**, *157*, A1016.
[29] a) C. O. Laoire, S. Mukerjee, K. M. Abraham, E. J. Plichta, M. A. Hendrickson, *J. Phys. Chem. C* **2009**, *113*, 20127; b) C. O. Laoire, S. Mukerjee, K. M. Abraham, E. J. Plichta, M. A. Hendrickson, *J. Phys. Chem. C* **2010**, *114*, 9178.
[30] M. J. Weaver, *J. Raman Spectrosc.* **2002**, *33*, 309.
[31] W. E. Geiger in *Laboratory Techniques in Electroanalytical Chemistry* (Eds.: P. T. Kissinger, W. R. Heineman), Marcel Dekker, New York, **1996**, pp. 683 – 717.
[32] A. J. Bard, L. R. Faulkner, *Electrochemical Methods: Fundamentals and Applications*, Wiley, New York, **2001**, chap. 12.
[33] S. A. Hunter-Saphir, J. A. Creighton, *J. Raman Spectrosc.* **1998**, *29*, 417.
[34] D. A. Hatzenbuhler, L. Andrews, *J. Chem. Phys.* **1972**, *56*, 3398.
[35] T. M. Loehr in *Oxygen Complexes and Oxygen Activation by Transition Metals* (Eds.: A. E. Martell, D. T. Sawyer), Plenum, New York, **1988**, pp. 17 – 32.
[36] H. H. Eysel, S. Z. Thym, *Z. Anorg. Allg. Chem.* **1975**, *411*, 97.
[37] a) S. A. Freunberger, L. J. Hardwick, Z. Peng, V. Giordani, Y. Chen, P. Maire, P. Novák, J.-M. Tarascon, P. G. Bruce, IMLB **2010** Abs# 830; b) F. Mizuno, S. Nakanishi, Y. Kotani, S. Yokoishi, H. Iba, *Electrochemistry* **2010**, *78*, 403; c) S. A. Freunberger, Y. Chen, Z. Peng, J. M. Griffin, L. J. Hardwick, F. Bardé, P. Novák, P. G. Bruce, *J. Am. Chem. Soc.* **DOI:** 10.1021/ja2021747.
[38] J.-M. Savéant, *J. Electroanal. Chem.* **2000**, *485*, 86.
[39] a) M. V. Mirkin, T. C. Richards, A. J. Bard, *J. Phys. Chem.* **1993**, *97*, 7672; b) D. Shoup, A. Szabo, *J. Electroanal. Chem.* **1982**, *140*, 237.
[40] P. Gao, D. Gosztola, L.-W. H. Leung, M. J. Weaver, *J. Electroanal. Chem.* **1986**, *233*, 211.
[41] F. La Mantia, F. Rosciano, N. Tran, P. Novák, *J. Appl. Electrochem.* **2008**, *38*, 893.

